

Water Resources Research®

RESEARCH ARTICLE

10.1029/2022WR032529

Key Points:

- I/I was a major component of the urban drainage budget as 35% of mean annual precipitation inputs
- Increased imperviousness and sewer density explained increased high flows, decreased intermediate flows, and faster rate of flow recession
- The recession of I/I possesses higher nonlinearity or convexity than streamflow

Supporting Information:

Supporting Information may be found in the online version of this article.

Correspondence to:

K. Zhang,
kzhang16@connect.hku.hk

Citation:

Zhang, K., Sebo, S., McDonald, W., Bhaskar, A., Shuster, W., Stewart, R. D., & Parolari, A. J. (2023). The role of inflow and infiltration (I/I) in urban water balances and streamflow regimes: A hydrograph analysis along the sewershed-watershed continuum. *Water Resources Research*, 59, e2022WR032529. <https://doi.org/10.1029/2022WR032529>

Received 6 APR 2022

Accepted 7 FEB 2023

Author Contributions:

Conceptualization: Kun Zhang
Data curation: Kun Zhang, Spencer Sebo
Formal analysis: Kun Zhang
Funding acquisition: Anthony J. Parolari
Investigation: Kun Zhang
Methodology: Kun Zhang
Project Administration: Anthony J. Parolari
Resources: Spencer Sebo, Walter McDonald, Anthony J. Parolari
Supervision: Anthony J. Parolari
Validation: Kun Zhang, Anthony J. Parolari
Visualization: Anthony J. Parolari
Writing – original draft: Kun Zhang
Writing – review & editing: Kun Zhang, Walter McDonald, Aditi Bhaskar, William Shuster, Ryan D. Stewart, Anthony J. Parolari

The Role of Inflow and Infiltration (I/I) in Urban Water Balances and Streamflow Regimes: A Hydrograph Analysis Along the Sewershed-Watershed Continuum

Kun Zhang¹ , Spencer Sebo¹, Walter McDonald¹ , Aditi Bhaskar^{2,3} , William Shuster⁴ , Ryan D. Stewart⁵ , and Anthony J. Parolari¹ 

¹Department of Civil, Construction, and Environmental Engineering, Marquette University, Milwaukee, WI, USA,

²Department of Civil and Environmental Engineering, Colorado State University, Fort Collins, CO, USA, ³Department of Civil, Environmental, and Architectural Engineering, University of Colorado, Boulder, CO, USA, ⁴Department of Civil and Environmental Engineering, Wayne State University, Detroit, MI, USA, ⁵School of Plant and Environmental Sciences, Virginia Tech, Blacksburg, VA, USA

Abstract Urbanization alters subsurface flow pathways through expansion of sanitary collection and conveyance infrastructure. Inflow and infiltration (I/I) into sewers redistributes slow subsurface flows to fast within-sewer flows. Acting in concert with connected surface water, redistribution through I/I complicates the net impact of urbanization on streamflow. Elucidation of these processes is key to the characterization and prediction of urban hydrologic cycles. In this study, we collected sanitary sewer flow and streamflow data from 17 sewersheds and 18 watersheds in and around Milwaukee, WI, USA. We compared flow duration curves and baseflow recession characteristics of I/I and streamflow in urban and reference watersheds. Median depth-normalized I/I (296 mm) was nearly 35% of mean annual precipitation (867 mm), and thereby a major component of the urban drainage budget. I/I flowrates were similar to urban streamflow during high flow events (10th percentile) and larger during intermediate (50th percentile) and low (90th percentile) flow events. Further, I/I recession was slower and more nonlinear in shape than urban streamflow. Increased imperviousness and sewer density were associated with increased high flows, decreased intermediate flows, and quicker streamflow recessions. Sewer density explained more variability in intermediate flows (35%) and baseflow recession rate (49%) than imperviousness (24% and 19% respectively). Based on our findings, I/I takes up valuable volume capacity in sewers, which leads to more frequent overflows and alters streamflow regimes with ecological implications. Thus, I/I should be better considered in the prediction of urban hydrologic fluxes, and the characteristics and hydro-ecologic impact of I/I should be more thoroughly explored.

Plain Language Summary Urbanization brings with it sanitary collection and conveyance infrastructure, which alters system capacities, water budgets, and streamflow hydrographs. One unique component of the urban water cycle is inflow and infiltration (I/I), wherein there are inputs to the collection system from runoff, and exchange between underground conveyances and soil water and groundwater. These I/I impacts remain unclear for urbanized watersheds-sewersheds. We examined and compared flow duration curves and baseflow recession characteristics of I/I, and streamflow in urbanized and minimally impacted reference watersheds. We found that I/I was 35 percent of the total urban water budget, with much of this contributing in the wet winter and spring seasons. Compared to streamflow, the hydrograph of I/I recessed more slowly and possessed a more convex shape. Although the amount of impervious area in a watershed is major contributor to inflows, we found that sewerage density had a comparable or even stronger influence on streamflow alteration. Based on our findings, I/I takes up valuable volume capacity in sewer systems, which can lead to more frequent overflows, and alters streamflow regimes with ecological implications. I/I should be better considered in urban water cycle, and the characteristics and hydro-ecologic impact of I/I should be better studied.

1. Introduction

Hydrology in urban areas is substantially altered by urbanization processes. Specifically, replacement of vegetated surfaces with impervious surfaces reduces infiltration and evapotranspiration losses and increases overland flow, concentrating and transforming slow environmental flows into fast stormflows (Finkenbine et al., 2000; Walsh et al., 2005). At the same time, urbanization involves intensive alteration to subsurface hydrology as pipes are constructed for efficient sanitary sewage and stormwater collection and conveyance (Oswald et al., 2023). A

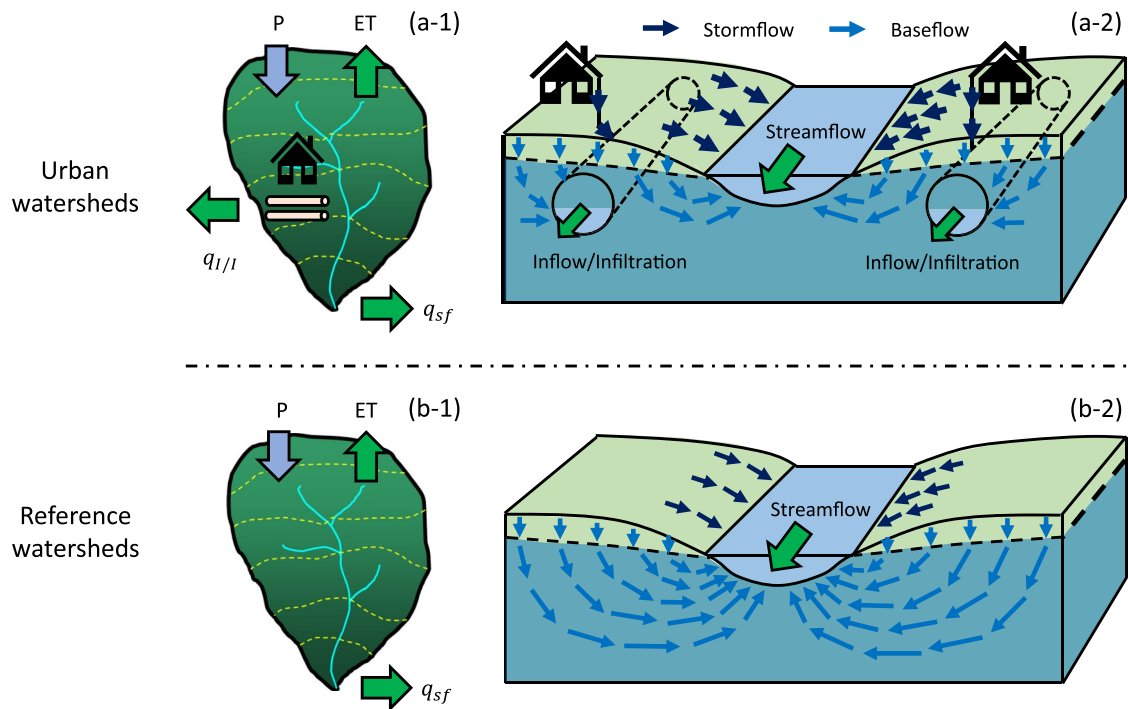


Figure 1. Water balance in (a-1) urban and (b-1) reference watersheds. Sources of streamflow in (a-2) urban and (b-2) reference watersheds considering inflow and infiltration (I/I) into sanitary sewers. P , ET , q_{sf} and $q_{I/I}$ respectively refer to precipitation, evapotranspiration, streamflow, and I/I. The schematic is modified from Winter et al. (1998).

combination of pipe infrastructure age and joint failure leads to additional volume inputs as inflow and infiltration (I/I). Direct inflows include illicit connections as well as directly connected stormwater drains (e.g., rooftop downspouts, foundation drains, and laterals directly connected to sanitary or combined sewers). The process of infiltration refers to soil moisture or groundwater that seeps into sewer systems through compromised joints, junctions and other breaches of pipe integrity (Figure 1) (Pawlowski et al., 2013; Vallabhaneni et al., 2008; Vanderlyn & Condren, 1990). Therefore, the factors contributing to I/I mean that it can be generated during both wetter and drier periods.

To date, I/I research has primarily focused within the context of water delivery to wastewater treatment plants (WWTPs). At the system level, I/I is an expensive operational problem associated with deteriorated sanitary sewers, occupying valuable flow and volume capacity, and increasing the peak flow and total volume of water treated at WWTPs (Dirckx et al., 2016; Ellis & Bertrand-Krajewski, 2010; Weiss et al., 2002). Previous studies reported that I/I accounted for 20%–55% of total water flow in separated sewer systems (Beheshti & Sægrov, 2018; Eiswirth & Hötzel, 1997; Pangle et al., 2022) and 14%–50% of total water flow in combined systems (Kracht et al., 2007; Prigiobbe & Giulianelli, 2009). While these prior studies have quantified I/I volumes and peak flows, few analyses have considered I/I as an integral component of urban watershed flow regimes, storage-discharge dynamics, and associated flow recession behavior (Bhaskar et al., 2015, 2016; Pangle et al., 2022; Zhang & Parolari, 2022).

The impacts of urbanization as imperviousness and sewerage density alter flow regimes, storage-discharge dynamics, and associated flow recession behavior, implicating I/I as playing a significant role. The impact of urbanization on quick flow as direct runoff from impervious area and runoff production is relatively well understood. Urbanization usually increases peak flow and results in flashier streamflow (Beighley et al., 2003; Debbage & Shepherd, 2018; Mejía et al., 2015; Rose & Peters, 2001). By contrast, the effect of urbanization on stream baseflow is much more complex, and findings have divergent conclusions (Bhaskar et al., 2016; Price, 2011; Walsh et al., 2005). There is evidence supporting both smaller and greater baseflow volume (Bhaskar et al., 2020), as well as slower (Rose & Peters, 2001; Wang & Cai, 2010) and faster (Bhaskar & Welty, 2012; Brandes et al., 2005; Burns et al., 2005; Konrad, 2016) baseflow recession in urban watersheds, when compared with non-urban watersheds. Flow recession behavior is derived from the storage-discharge properties and network structure of the watershed and characterizes the baseflow dynamics (Biswal & Marani, 2010, 2014; Sánchez-Murillo

et al., 2015; Wittenberg & Sivapalan, 1999). Because urban drainage systems dissect the subsurface and alter the storage-discharge properties and network structure of the watershed, it is plausible that I/I imposes a detectable signature on flow regimes and baseflow recession behavior.

Differences in infiltration, evapotranspiration (ET), and groundwater storage in urban watersheds have been cited to explain observed differences in urban and natural stream baseflow volumes and recession rates (O'Driscoll et al., 2010). For example, increased imperviousness can lead to a decline in annual volume and ratio of stream baseflow (Haase, 2009; Hardison et al., 2009). Further, ET is lower in urban watersheds due to extensive removal of vegetation and consequent change in heat balance and albedo (Barron et al., 2013; Grimmond & Oke, 1991). Yet, some exceptions have been noted due to extensive urban irrigation (Grimmond & Oke, 1999; Kokkonen et al., 2018). Decreased ET results in longer retention of soil water and may contribute to an apparent lower stream baseflow recession rate (Rose & Peters, 2001). On the other hand, faster stream baseflow recession has been attributed to artificial outflows in urban watersheds, such as groundwater pumping and I/I. I/I directs a portion of infiltrated stormwater and groundwater into sanitary sewer systems, decreasing baseflow to streams (Braud et al., 2013; Pangle et al., 2022) and increasing the subsurface storage depletion rate (Bonneau et al., 2018; Price, 2011; Simmons & Reynolds, 1982) (Figure 1). Other factors suggest that I/I affects the flow regimes and baseflow recession of urban streams. First, direct inflows of I/I originate only from urbanized locations in the watershed (e.g., rooftops and foundation drains) that are directly connected to the sanitary sewers (Pawlowski et al., 2013). Thus, the drainage areas of surface and subsurface I/I flows may differ. Second, the baseflow recession behaviors of I/I can differ from urban streamflow because sanitary sewers and streams drain different geophysical environments. The soil hydraulics and their level of heterogeneity near sanitary sewers are likely different from other urbanized areas due to anthropogenic activities (Herrmann et al., 2018; Sharp, 2010). Thus, it is worthwhile to compare the flow regimes and baseflow recession behaviors between I/I and urban streamflow.

The overarching goal of this study was to improve understanding of the role and dynamic of I/I in the urban water cycle and streamflow regimes. To address this goal, we performed comparative hydrograph analyses based on streamflow and sanitary sewer flow in collocated urbanized and nearby reference watersheds. First, we separated I/I from sanitary sewer flow automatically based on autoregressive modeling and recursive digital filters. We then combined this estimate of I/I with nearby streamflow records to determine: (a) What fraction of the urban water balance is discharged through I/I?; (b) How do the flow regimes and baseflow recession of I/I compare to that of streamflow?; and (c) How does I/I affect the flow regimes and baseflow recession in urban streams compared to land cover change?

2. Methodology

2.1. Study Area and Data

The study was conducted in several coastal watersheds that drain to Lake Michigan from the City of Milwaukee and its suburbs. We selected 17 sewersheds in Milwaukee County for I/I analysis (Figure 2). The sewersheds were defined by MMSD based on the understanding that all sewers, in this case only separate sanitary sewers, drain to a certain outlet. Sewer flow data measured at the outlet of these sewersheds was obtained from MMSD for the period 1 January 2014–31 July 2019. The flow was measured using ultrasonic or magnetic flow meters in 15 sewersheds. For the remaining 2 sewersheds, water level was recorded and transformed into flow rate based on Manning's equation. All data were logged at an hourly frequency. These sewersheds were selected because reliable continuous sanitary sewer flow data were available. In addition, they were served by separate sanitary sewer systems during the entire period of record and each of them has a distinguishable contributing area. Other sewersheds without a distinguishable contributing area due to interaction with the inline underground storage system were filtered out. Unlike other sewer service areas where sanitary sewer flow is discharged back to streams after treatment, the sanitary sewer flow in Milwaukee was treated by two different WWTPs, both of which discharged into Lake Michigan (Figure 2). Therefore, I/I that is conveyed to the WWTPs from the sewersheds did not contribute to the measured streamflow in Milwaukee. Based on local boring logs retrieved from the Bureau for Remediation and Redevelopment Tracking System (BRRTS) data set (DNR, 1999), the predominant soil type in these sewersheds was silty clay, and the groundwater table was shallow at 0–4 m below ground surface.

We selected 18 watersheds in and near Milwaukee, Wisconsin for comparison to sanitary sewer flows (Figure 2). These included 9 watersheds (i.e., CCC, MRC, MRMF, LMF, LMM, RRCF, BRD, FRW, and MRM) that we categorized as minimally impacted, and then 9 urbanized watersheds (i.e., LCM, UCW, HCW, MRW, WPCM,

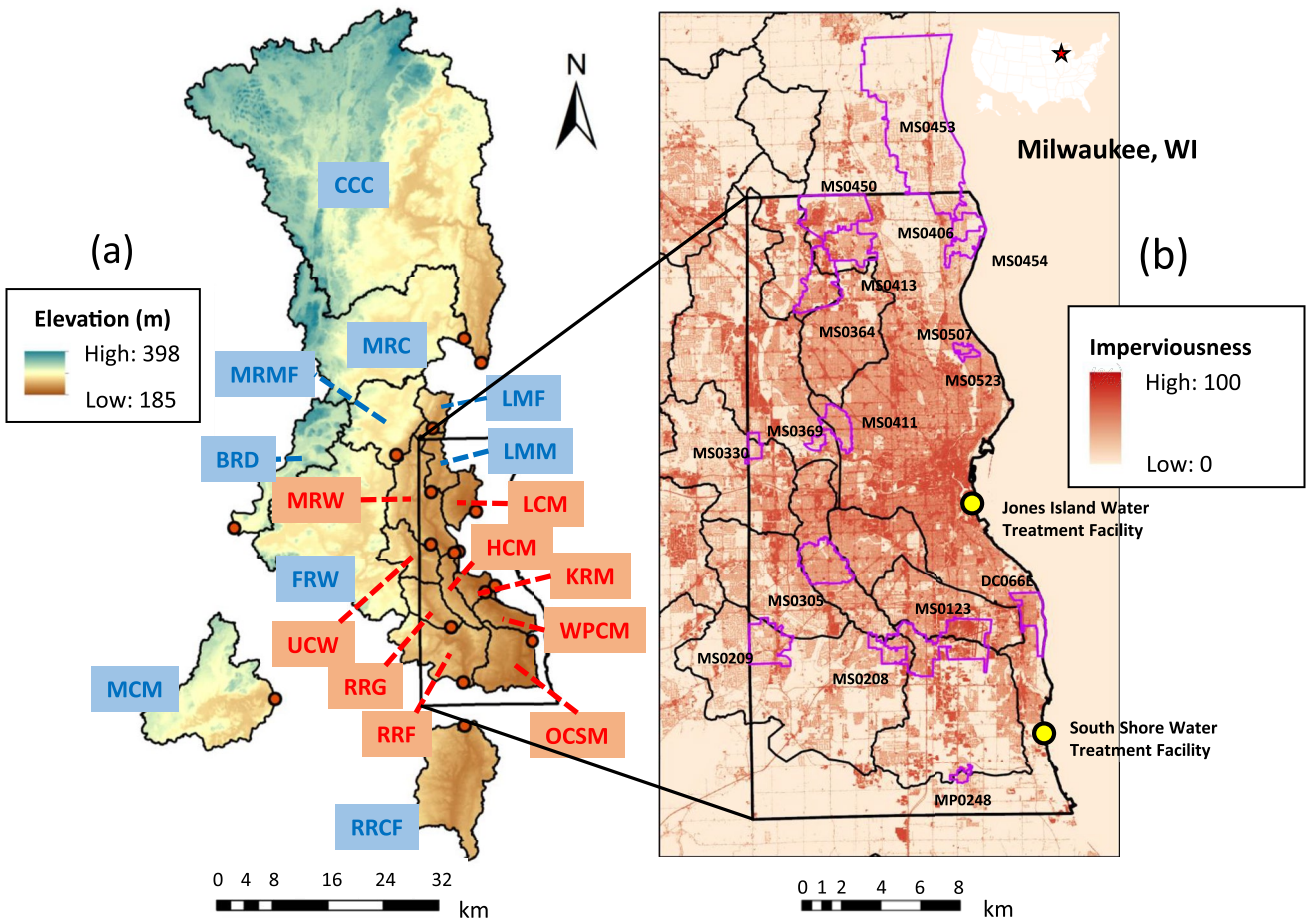


Figure 2. Location of the study areas including (a) watersheds and streamflow stations and (b) sewersheds. In (a), watersheds with blue texts refer to reference watersheds, while watersheds with red texts refer to urban watersheds. In (b), outlines in blue refer to the sewersheds, and the yellow dots refer to the two wastewater treatment facilities.

KRM, OCSM, RRG, and RRF; Table 1). The minimally impacted watersheds serve as a reference to compare against urban watersheds collocated with sanitary sewersheds. In addition, the 18 minimally impacted and urban watersheds together form a gradient of imperviousness. The urban watersheds are close to the sewersheds. Among the 17 sewersheds, 6 of them lie within the urban watersheds (e.g., MS0208 and MS0209 in RRF, MS0369 in MRW, MS0330 in UCW, MS0123 in OCSM and WPCM, and MS0305 in HCW), while the others are either partially intersected with or close to these urban watersheds. Note the size of the sewersheds is generally smaller than the watersheds.

The watershed boundaries were delineated based on the 10-m resolution Digital Elevation Model (DEM) after determining the flow direction and flow accumulation treating the streamflow stations as the outlets of the watersheds (Figure 2a). These watersheds were selected because they represent streamflow across a range of imperviousness (3.8%–54.7%) and they belong to the same (i.e., Unit 04040003) or similar (i.e., Unit 04040002, 07090001, and 07120006) hydrologic units as that of the sewersheds. The streamflow data between 1 January 2014 and 31 July 2019 was retrieved from the United States Geological Survey (USGS) daily streamflow data set (United States Geological Survey, 2019). Percent imperviousness data was retrieved from the 10-m resolution 2019 National Land Cover Database (Dewitz & U.S. Geological Survey, 2021), and the digitized sanitary sewer system data was retrieved from MMSD. Since a digitized sanitary sewer layout was only available within the city of Milwaukee, the density of sanitary sewers was calculated only for the 9 urbanized watersheds within the city limits (i.e., RRF, MRW, UCW, OCSM, RRG, LCM, HCW, KRM, and WPCM). Watershed geophysical properties are summarized in Table 1 and sewersheds in Table 2. Sanitary sewer networks are illustrated in Supporting Information S1 (Figure S1).

Table 1

Properties of Reference Watersheds, Urban Watersheds and Sewersheds, Including Area, Imperviousness, Ground Surface Slope, Stream Channel Density, and Sanitary Sewer Drainage Density

Watershed type	Streamflow station ID	Watershed	Area (km ²)	Imperviousness (%)	Mean slope (%)	Stream density (km ⁻¹)	Sewer density (km ⁻¹)
Reference watersheds	04086600	Milwaukee River near Cedarburg (MRC)	1,572.1	3.8	7.9	0.58	–
	05544200	Mukwonago River at Mukwonago (MRM)	191.9	4.0	7.7	0.52	–
	04087233	Root River Canal near Franklin (RRCF)	147.6	4.2	4.5	0.88	–
	04086500	Cedar Creek near Cedarburg (CCC)	310.8	4.9	6.0	0.87	–
	04087050	Little Menomonee River near Freistadt (LMF)	20.7	5.6	5.3	0.87	–
	05426067	Bark River at Delafield (BRD)	93.0	10.0	7.3	0.65	–
	04087030	Menomonee River at Menomonee Falls (MRMF)	89.9	18.2	5.3	1.15	–
	04087070	Little Menomonee River at Milwaukee (LMM)	51.0	21.0	4.9	0.88	–
	05543830	Fox River at Waukesha (FRW)	326.3	20.2	6.9	0.94	–
Urbanized watersheds	04087220	Root River near Franklin (RRF)	127.4	28.7	5.5	1.06	10.6
	04087120	Menomonee River at Wauwatosa (MRW)	318.6	29.5	5.4	0.88	7.7
	04087088	Underwood Creek at Wauwatosa (UCW)	46.9	34.4	5.9	0.79	8.1
	04087204	Oak Creek at South Milwaukee (OCSM)	64.7	34.9	4.2	1.20	6.8
	04087214	Root River at Grange Avenue at Greenfield (RRG)	38.1	37.4	5.6	0.90	14.6
	040869416	Lincoln Creek at Sherman Boulevard (LCM)	35.0	47.6	3.3	0.41	16.4
	04087119	Honey Creek at Wauwatosa (HCW)	26.7	52.4	4.4	0.57	24.8
	04087159	Kinnickinnic River at S. 11th Street (KRM)	48.7	54.4	4.7	0.74	15.8
	040871488	Wilson Park Creek at Milwaukee (WPCM)	29.4	54.7	4.1	0.78	12.9

Table 2

Properties of Urban Sewersheds, Including Area, Imperviousness, Ground Surface Slope, and Sanitary Sewer Drainage Density

Sewershed ID	Neighborhood	Area (km ²)	Imperviousness (%)	Mean slope (%)	Sewer density (km ⁻¹)
MS0453	Bayside	45.62	13.45	4.71	8.20
MS0454	Fox Point	2.56	17.75	6.77	27.89
MS0406	Bayside	2.24	18.24	5.35	23.64
MS0369	Wauwatosa	0.78	25.24	6.38	9.56
MS0330	Wauwatosa	1.37	29.51	5.57	11.37
MS0209	Hales Heights	5.85	30.95	4.42	24.68
MS0208	Greendale	2.07	33.24	3.52	25.11
DC066E	Cudahy	3.97	38.55	8.03	18.35
MS0450	Brown Deer	8.87	39.46	5.06	9.52
MP0248	Oak Creek	0.72	39.93	3.46	22.60
MS0413	Brown Deer	5.54	40.62	3.55	27.25
MS0523	Whitefish Bay	0.43	44.07	3.19	43.98
MS0507	Whitefish Bay	0.57	44.68	1.08	50.17
MS0411	Wauwatosa	3.38	46.11	5.67	16.82
MS0364	Land Bank	7.11	46.77	3.78	17.99
MS0305	Greenfield	6.81	49.97	3.98	14.99
MS0123	Airport	13.08	54.25	3.70	7.19

2.2. Separation and Quantification of I/I

Measured sanitary sewer flows were separated into base wastewater flow (BWF), and I/I, which is the sum of rainfall-derived I/I (RDII) and groundwater infiltration (GWI). RDII refers to quick flows that originate from direct inflows and relatively fast subsurface infiltration (e.g., unsaturated flows), while GWI refers to slower groundwater infiltration originating mainly from saturated groundwater flows. An automatic approach was used to separate I/I from sanitary sewer flow based on autoregressive modeling and recursive digital filters (Figure 3). Similar methods were applied in baseflow separation (Arnold et al., 1995; Eckhardt, 2005). After filling the data gaps using autoregressive modeling, the local minima and maxima were identified (Process 1), and the dry- and wet-weather periods were identified based on the distribution of flow values at local minima (Process 2); components of sewer flow were thereby separated. The local minima and maxima were not identified for every 24-hr period strictly, but the average distance between local minima identified ranged from 10 to 30 hr with an average of 22 hr (close to 24 hr). During dry periods, the baseflow, that is, BWF plus GWI, was assumed to be equal to the measured flow, while RDII was assumed to be zero. During wet periods, the baseflow was estimated through autoregressive modeling based on the baseflow during the dry periods and the quick flow was obtained by subtracting the estimated baseflow from the total sewer flow (Process 3). Next, the components of baseflow (i.e., BWF and GWI) were separated from the combined baseflow hydrograph using a three-iteration, forward-backward recursive digital filter (Process 4). Finally, total I/I was obtained by adding GWI to quick flow (i.e., RDII) (Process 5) (Figure 3). To be consistent with the streamflow time-series, the delineated hourly scale

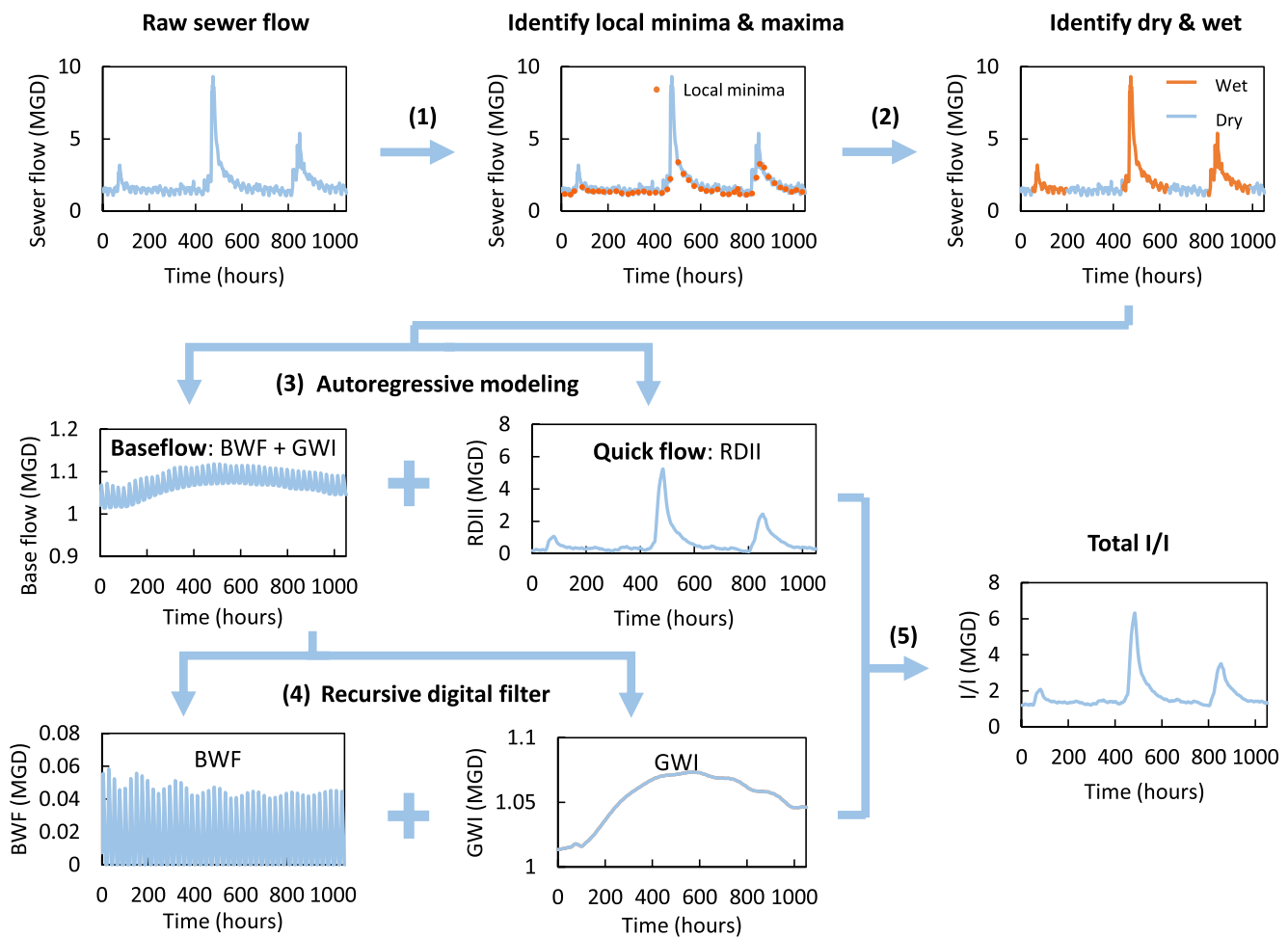


Figure 3. Process for separating rainfall derived inflow and infiltration from sanitary sewer flow. Rainfall-derived I/I, base wastewater flow and groundwater inflow are respectively represented as RDII, BWF, and GWI. The flow data used in the plots is from 25 March to 8 May 2014 at sewershed DC066E.

total I/I time-series was aggregated into a daily timescale. The details of the separation method can be found in Supporting Information S1 (Text S2). The separated dry and wet periods are shown in Supporting Information S1 (Figure S2), and the separated I/I records are shown in Supporting Information S1 (Figure S3).

This approach differs from other I/I identification methods (Bentes et al., 2022; Pangle et al., 2022) in two ways. First, BWF was interpolated here using autoregressive modeling rather than moving average. Second, wet periods were identified based on the flow data and not corresponding precipitation measurements (Figure 3). A hydrograph-based approach for I/I estimation was utilized (instead of based on precipitation) here because there was significant spatial variability in precipitation in the study area and nearby precipitation gages were not available for all sewersheds analyzed.

2.3. Hydrologic Analysis

The water depths, flow regimes, and baseflow recession behavior of I/I in sewersheds were compared with those of streamflow in watersheds. Each sewershed and watershed is treated as an individual hydrologic entity with its unique geophysical conditions and governing hydrologic processes—which include general patterns that the sewersheds are smaller and have greater sewer pipe densities than the overall watersheds. The comparisons were feasible because the compared parameters either had the same units or were dimensionless. The details of each category of calculation and comparison are illustrated in the sub-sections below.

I/I and streamflow volumetric flow rates were normalized by the corresponding areas (sewershed areas for I/I and watershed areas for streamflow). The area-normalized flow rates were termed as fluxes throughout the paper.

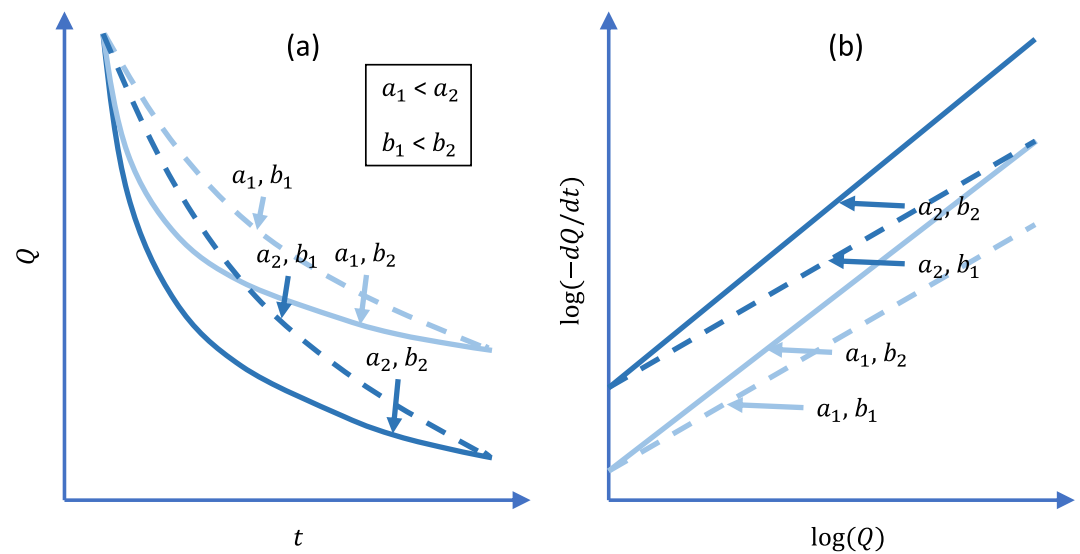


Figure 4. Theoretical patterns of (a) flow recession hydrograph (i.e., Q against t) and (b) flow recession plot showing $\log(-dQ/dt)$ against $\log(Q)$ with different recession parameters (i.e., a and b). The flow recession is quicker with larger a value (i.e., a_1 vs. a_2); the flow recession becomes more non-linear with larger b value (i.e., b_1 vs. b_2).

We acknowledge that some flows that originate outside of the sewersheds (e.g., lateral groundwater recharge, inter-sewershed water transfer, artificial irrigation, and leakage from water distribution systems) could contribute to I/I . More details of the rationale of area-normalization can be found in Supporting Information S1 (Text S4).

2.3.1. Water Balance

Monthly and annual area-normalized depths of I/I and streamflow were calculated from individual fluxes. Flow depths were compared to precipitation depth assuming that precipitation was spatially uniform over the sewershed and watershed areas.

2.3.2. Flow Duration Curves

Flow duration curves (FDCs) and flow percentiles were used to quantify and compare the flashiness of I/I and streamflow regimes. Quick (i.e., low exceedance probability such as Q_{10}), intermediate (i.e., medium exceedance probability such as Q_{50}), and slow (i.e., high exceedance probability such as Q_{90}) components of FDCs were compared between I/I and streamflow. Groundwater inflow was included in I/I to generate the FDCs. The slope of the FDC between 20% and 80% exceedance probabilities was calculated as an estimate of flow stability. A larger FDC slope indicates more variable flow that is largely regulated by quick runoff following rain events, while a smaller FDC slope indicates the predominance of groundwater discharge (Searcy, 1959).

2.3.3. Baseflow Recession

Baseflow recession parameters were estimated from the flow recession curves to infer storage-discharge properties from the I/I and streamflow fluxes. Assuming the aquifer as a nonlinear reservoir, flow recession can be represented as (Brutsaert & Nieber, 1977),

$$\frac{dQ}{dt} = -aQ^b \quad (1)$$

where Q is the flux rate for either I/I or streamflow with units of $LT^{-1} L^3T^{-1}$; and a and b are dimensionless recession parameters. As shown in Figure 4, a represents the recession rate of the flux, such that larger values indicate faster recession; and b refers to the linearity of the recession, in which $b = 1$ refers to linear recession, while $b > 1$ refers to nonlinear recession (Figure 4a). A larger b refers to a more nonlinear or convex recession curve, reflecting a more nonlinear storage-discharge watershed property. $\log(a)$ and b are the respective intercept and slope of the log-transformed relationship between the time-derivative of flux rate ($-dQ/dt$) and flux rate (Q) (Figure 4b).

An event-based recession analysis approach was adopted in which a and b were calculated for every recession event. The “lumped” approach, in which one value of a and b is calculated using all events, can underestimate the

b value (Biswal & Marani, 2010; Dralle et al., 2017). Recession events were identified based on the sign of the flux rate time-derivative ($-dQ/dt$). A recession event was assumed to start when dQ/dt turned from positive to negative and to end when dQ/dt turned from negative to positive. During each event, the values of Q and dQ/dt were computed with a 3-day moving window for both I/I and streamflow.

A restrictive approach was adopted to filter rainfall-derived quick flow. First, the minimum allowable length of a recession event was assigned to be 4 days, meaning that recession events shorter than 4 days were filtered out. Second, a parametric threshold of 20 was used to filter out small recession events with low peak flows. Third, the recession event was assumed to begin 2 days after peak flow. These thresholds were applied to both I/I and streamflow. Nonlinear fitting was then performed to obtain the event-scale recession parameters a and b . The moving window size for calculating Q and dQ/dt and the three thresholds for filtering recession events and calculating recession parameters were determined by one-at-a-time local sensitivity analysis. For each set of analysis, the target parameter was perturbed within a certain range while the others were kept unchanged. The variation ranges were respectively 1–8 days for the moving window size, 1–8 days for the minimum allowable length of a recession event, 10–400 for the parametric threshold representing minimum peak flow before a recession event, and 1–8 days for the lag of recession event after peak flow. Details about these thresholds and the sensitivity analysis regarding the selection of optimal thresholds can be found in Supporting Information S1 (Text S3, Figures S7–S14).

2.3.4. Statistical Analysis

To investigate the impact of imperviousness and subsurface drainage via I/I on stream flow regimes and recession, correlations were computed between flow parameters (i.e., Q_{10} , Q_{50} , Q_{90} , recession slope, a , and recession exponent, b) and watershed properties (i.e., imperviousness and sanitary sewer density). The analysis on imperviousness was performed on both reference and urbanized watersheds, whereas the analysis on sanitary sewer density was only performed on urbanized watersheds due to availability of digitalized sewer data. The coefficient of determination (R^2) was used to represent the goodness of fit.

The collinearity of imperviousness and sanitary sewer density was tested using the Pearson's r correlation coefficient and variance inflation factor (VIF). VIF quantified the percentage inflation in variance if there was no multicollinearity (Kroll & Song, 2013). The Pearson's r correlation coefficient between imperviousness and sanitary sewer density was 0.71 with $p < 0.05$ and the VIF was 2.0, indicating moderate collinearity. Thus, dominance analysis was further performed to quantify the relative importance of imperviousness and sanitary sewer density on the recession parameters (Budescu, 1993).

For two independent variables X_1 and X_2 (referring to imperviousness and sanitary sewer density here) and one dependent variable (referring to Q_{10} , Q_{50} , Q_{90} or recession parameters, either a or b), the conditional dominance is defined as the change in R^2 resulting from adding a predictor to all possible subset regression models. The conditional dominance of X_i ($C_{X_i}^{(k)}$), which refers to the mean usefulness of X_i when it is added to k additional variables, was calculated as,

$$C_{X_i}^{(k)} = \frac{\sum (R_{Y|X_i X_h}^2 - R_{Y|X_h}^2)}{\binom{p-1}{k}} \quad (2)$$

where X_h is any subset of k independent variables, and X_i is independent variable that is excluded. Y is the dependent variable, and p is the total number of predictors. Then, the general dominance weight of each predictor was obtained through averaging the conditional dominance across all the possible models (Equation 3),

$$C_{X_i} = \frac{\sum_0^k C_i^{(k)}}{k+1} \quad (3)$$

As a supplement to the regression analysis, dominance analysis can de-emphasize redundant predictors when multicollinearity is present (Kraha et al., 2012), and, thus, it can reduce the impact of collinearity between independent variables and better represent the statistical contribution of independent variables.

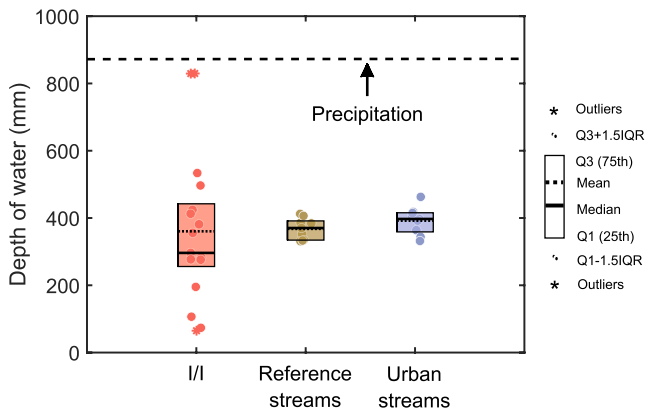


Figure 5. Annual depths of inflow and infiltration (I/I) and streamflow in urban and reference watersheds relative to precipitation. Each dot represents the annual depths of I/I or streamflow over the period in a sewershed or watershed. $Q1$ and $Q3$ refer to the 25th and 75th percentiles of the data. IQR refers to interquartile range ($Q3-Q1$). The outliers are values that are located outside 1.5 times IQR above $Q3$ or below $Q1$.

3. Results

3.1. I/I Flux Relative to Rainfall-Runoff Partitioning in Urban and Reference Watersheds

We found that I/I was a major component of the water balance, with annual depth of I/I at a median of 296 mm and a mean of 360 mm (range 65–830 mm) (Figure 5). Median and mean I/I depths were on the same order of magnitude as the depths of precipitation (867 mm) and streamflow (332–462 mm). The ratio of I/I to precipitation had a median of 0.34 and a mean of 0.42 (range 0.08–0.97); and the ratio of I/I to the mean streamflow in the nine urban watersheds had a median of 0.76 and a mean of 0.92 (range 0.17–2.12). It should be noted that an I/I-to-precipitation ratio of 0.9 does not mean that 90% of precipitation becomes I/I. Apart from precipitation, I/I may originate from irrigation or groundwater inflow from soil profile storage or leaky water distribution pipes. We also remind the reader that the streamflow was normalized by watershed area whereas I/I was normalized by the sewershed area, so the two areas were not equal. It was not possible to calculate I/I across the entire urban watersheds with the data provided. Because of this area mismatch, the depth of I/I and the corresponding ratios to precipitation and/or streamflow are likely smaller since the density of sanitary sewer pipes was generally lower at the watershed scale than at the sewershed scale

considered here. More details of the interpretation of the I/I flux in urban water balances can be found in Supporting Information S1 (Text S5).

The seasonal patterns of I/I and streamflow were similar, the monthly I/I and streamflow depths were greatest during the spring months (i.e., March–June) (Figure 6a). I/I-to-precipitation and I/I-to-streamflow ratios were greatest during the winter (i.e., November–March) and smallest during the summer and early fall (i.e., June–October) (Figures 6b and 6c). The median ratios of I/I to precipitation were 0.75 in January and 0.20 in August. The median ratios of I/I to the mean urban streamflow were 1.32 in January and 0.72 in August.

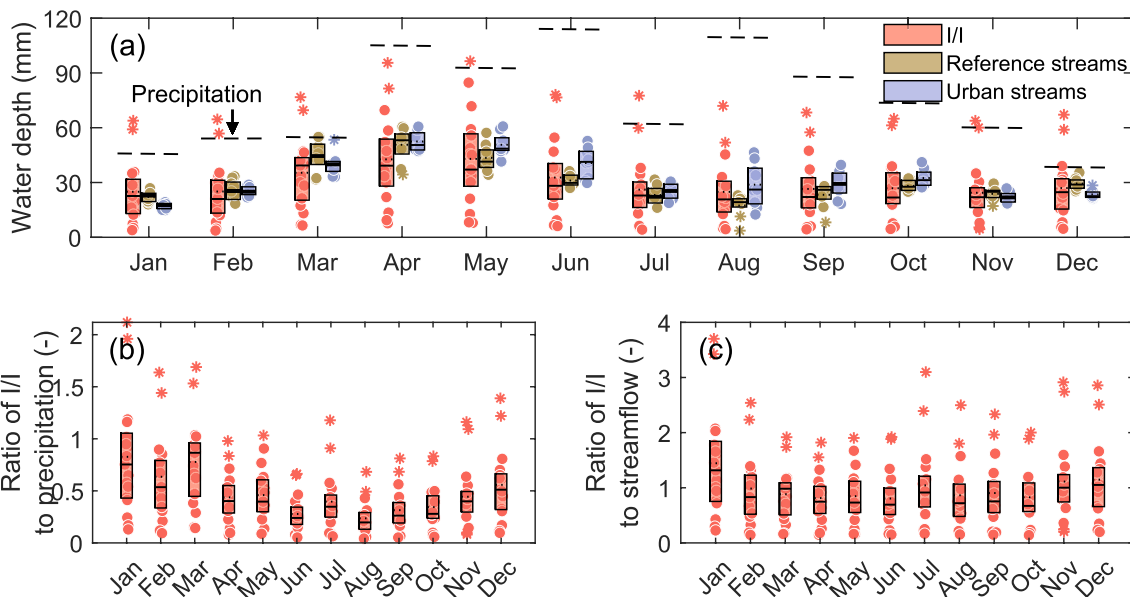


Figure 6. Seasonal patterns: (a) Monthly depths of I/I and streamflow in urban and reference watersheds related to precipitation; (b) Ratio of I/I to precipitation; (c) Ratio of I/I to mean streamflow in urban watersheds. Each dot in panel (a) represents the mean monthly depths of I/I or streamflow over the period in a sewershed or watershed. Each dot in panel (b and c) represents the mean values over the period in a sewershed.

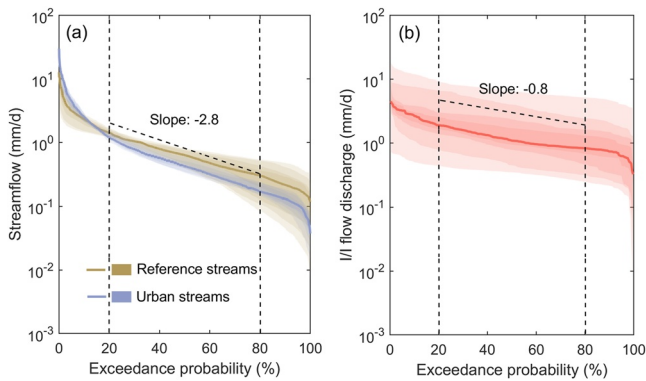


Figure 7. Flow duration curves of (a) streamflow in urban and reference watersheds and (b) inflow and infiltration (I/I) in urban sewersheds. The central flow lines represent the median values; and the shaded areas correspond to different percentiles, including <25th, 25th–50th, 50th–75th, and 75th–90th percentiles.

3.2. I/I Flow Regimes

I/I flow regimes, quantified by the FDC and flow percentiles, were markedly different from streamflow regimes in both urban and reference watersheds. As expected, the FDCs of streamflow in urban watersheds were steeper than those in reference watersheds.

The FDC slope for I/I was less than that for streamflow (Figure 7). The median FDC slope for I/I was -0.8 , while that for streamflows was -2.8 . This suggests that I/I fluxes were more temporally stable than streamflows, indicating a larger groundwater contribution.

High (Q_{10}) I/I fluxes were lower than corresponding streamflows, while intermediate (Q_{50}) and low (Q_{90}) I/I fluxes were greater than streamflows (Figure 8a). Specific comparisons showed that, across all watersheds, high I/I fluxes were lower than the high streamflows in both urban ($p = 0.01$) and reference streams ($p = 0.07$). Median I/I fluxes were greater than streamflow in urban streams ($p = 0.01$), but were indistinguishable from streamflow of reference streams ($p = 0.37$). The Q_{90} I/I flux were larger than those in urban ($p < 0.01$) or reference streams ($p = 0.09$).

At the same time, the spatial and temporal variabilities of I/I and streamflow differed from each other. I/I was more variable spatially across sewersheds than streamflow in both urban and reference watersheds. The intermediate fluxes (Q_{50}) for streamflow varied between 0.3 – 0.8 mm/d, whereas the median I/I fluxes varied between 0.15 and 2.27 mm/d (Figure 8a). Results were similar for low and high flows. However, I/I was less variable temporally within each sewershed. The CV for I/I (0.30 – 1.00 mm/d) was significantly lower than that for urban (1.46 – 2.45 mm/d) and reference (0.50 – 1.89 mm/d) watersheds with Kruskal-Wallis one-way ANOVA test's values ≤ 0.01 (Figure 8b).

3.3. I/I and Streamflow Recession Characteristics

Baseflow recession rates, quantified by a values, varied across the three flow signals—urban stream recession was fastest and I/I recession was slowest. Stream baseflow recession was faster (greater a values) for urban watersheds compared to reference watersheds and I/I (Figure 9a); median event-scale a values were 0.15 – 0.34 for

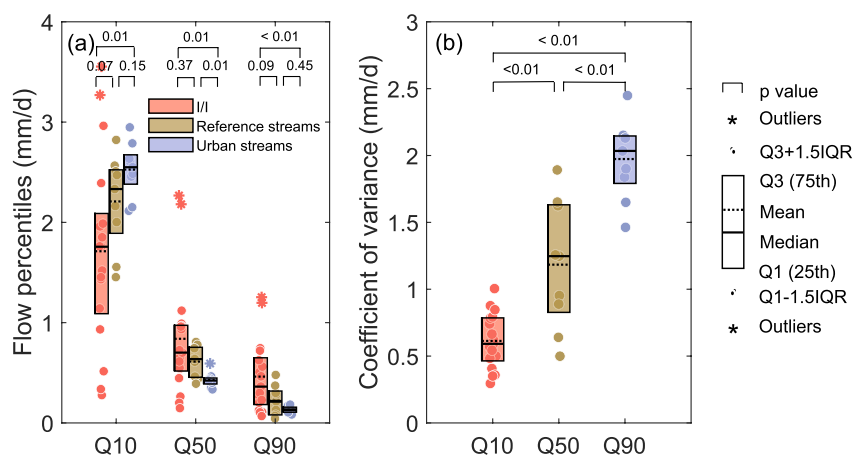


Figure 8. Comparison of flow duration curve indices between inflow and infiltration (I/I) and streamflow for the study period (January 2014–July 2019). Panel (a) shows distributions of Q_{10} , Q_{50} , and Q_{90} values across sites, which respectively refer to flow rate with exceedance probability of 10%, 50%, and 90%. Panel (b) shows the distributions of coefficient of variation of flow rates calculated at each individual site. Each dot represents flow indices in a sewershed or watershed. The numbers shown at top between two boxes refer to the p values from Kruskal-Wallis ANOVA test, which represent the level of statistical significance between the corresponding two groups of data. Q_1 and Q_3 refer to the 25th and 75th percentiles of the data. IQR refers to interquartile range (Q_3 – Q_1). The outliers are values that are located outside 1.5 times IQR above Q_3 or below Q_1 .

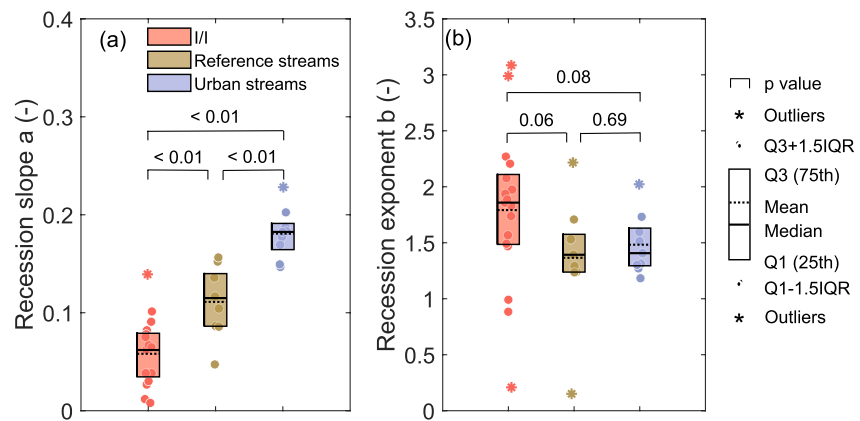


Figure 9. Distributions of the recession slope, a , and recession exponent, b , for inflow and infiltration (I/I) and streamflow. Panel (a) includes median event-scale values, where each dot represents the median value over all recession events in a sewershed or watershed, while (b) includes all the event-scale data. The numbers shown at top between two boxes refer to the p values from Kruskal-Wallis ANOVA test, which represent the level of statistical significance between the corresponding two groups of data. Q_1 and Q_3 refer to the 25th and 75th percentiles of the data. IQR refers to interquartile range ($Q_3 - Q_1$). The outliers are values that are located outside 1.5 times IQR above Q_3 or below Q_1 .

urban watersheds, 0.05–0.16 for reference watersheds; and 0.01–0.14 for I/I. All pairwise comparisons showed significant differences in median a values (Kruskal-Wallis ANOVA test; $p < 0.01$).

The nonlinearity of baseflow recession, quantified by b values, varied across the three flow signals—the I/I recession was the most nonlinear (greater b values) and that of reference streamflow was the least nonlinear. Baseflow recession was more nonlinear for I/I compared to both urban and reference watersheds (Figure 9b). The median event-scale b values for I/I were 0.21–3.09, which were significantly larger than that of both types of streams ($p = 0.08$ and 0.06 respectively for urban and reference streams). The median event-scale b values were 1.18–2.02 for urban watersheds and 0.98–2.22 for reference watersheds and the difference was not significant ($p = 0.69$).

3.4. Imperviousness and Sewer Density Controls on Streamflow Regime and Baseflow Recession

Streamflow was flashier (greater high flows but lower intermediate and low flows) in watersheds with higher imperviousness and higher sewer density (Figure 10 and Table 3). High flows (Q_{10}) increased significantly with imperviousness ($R^2 = 0.38$, $p < 0.01$) and sewer density ($R^2 = 0.61$, $p = 0.013$). Considering imperviousness and sewer density together explained more of the variability in Q_{10} than either variable independently ($R^2 = 0.74$, $p = 0.018$ for the combined model). Intermediate flows (Q_{50}) decreased significantly with imperviousness ($R^2 = 0.37$, $p < 0.01$) and sewer density ($R^2 = 0.55$, $p = 0.02$). The model was moderately improved with both variables ($R^2 = 0.59$, $p = 0.017$ for the combined model). Low flows (Q_{90}) were insensitive to both imperviousness and sewer density. Imperviousness and sewer density together explained 30% of the variance in Q_{90} , but the relationships were not significant.

Imperviousness and sewer density contributed equally to Q_{10} , while sanitary sewer density was more important for Q_{50} . Imperviousness and sanitary sewer density explained 39.1% and 34.5% of the variance in Q_{10} (Figure 10g), and 23.7% and 35.0% of the variance in Q_{50} (Figure 10h), respectively.

Baseflow recession was quicker (greater a values) in watersheds with higher imperviousness or higher sewer density (Figure 11, Table 3). The recession slope a increased significantly with imperviousness across all watersheds ($R^2 = 0.65$, $p < 0.01$). For urban watersheds only, the recession slope a increased significantly with sewer density ($R^2 = 0.67$, $p < 0.01$) and marginally significantly with imperviousness ($R^2 = 0.37$, $p = 0.08$). The regression model for a in urban watersheds did not improve when both variables were included ($R^2 = 0.68$, $p = 0.034$ for the combined model). Sewer density was more important than imperviousness for explaining the recession rate. Imperviousness and sanitary sewer density respectively explained 18.8% and 48.8% of the variance in a (Figure 11e).

Baseflow recession was more nonlinear (i.e., greater b value) in urban watersheds with both higher imperviousness and higher sewer density (Figure 11, Table 3). The recession nonlinearity b was not significantly related to

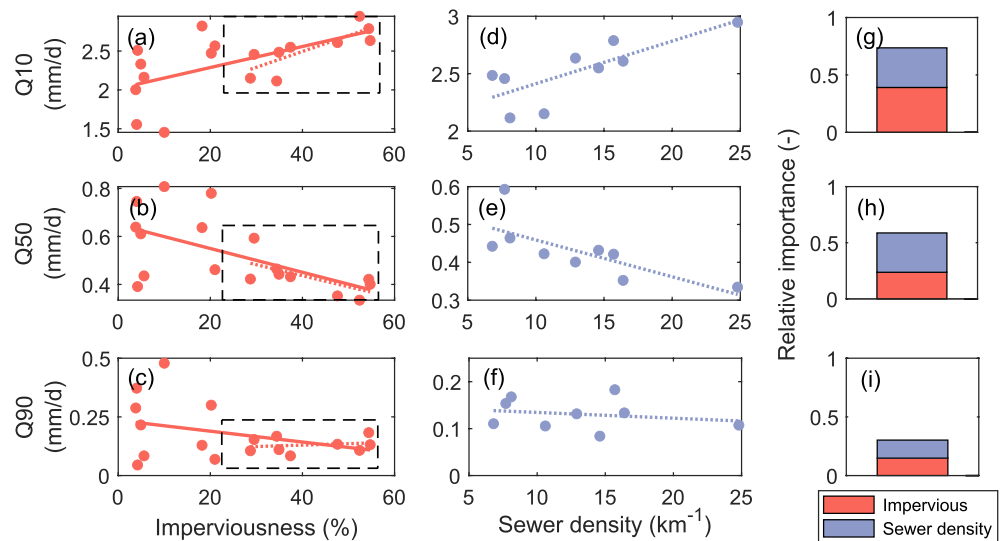


Figure 10. Relationship between watershed variables, that is, (a–c) imperviousness and (d–f) sanitary sewer density, and streamflow regimes, that is, (a, d) Q_{10} ; (d, e) Q_{50} ; and (c, f) Q_{90} . Panels (a–c) include all watersheds; (d–f) include the 9 urban watersheds with digitized sanitary sewer network data, denoted by the black rectangles in panels (a–c). Panels (g–i) show the variance of correlation attributed to imperviousness and sanitary sewer density based on dominance analysis performed solely on 9 urban watersheds.

imperviousness or sewer density alone. However, in urban watersheds imperviousness and sewer density together explained 61% of the variance in b , and the relationship was marginally significant ($p = 0.059$).

4. Discussion

4.1. Infrastructure Flows in Urban Water Balances

Our results show that estimates of subsurface water fluxes such as I/I are generally necessary to understand the key processes in urban water balances and to fully characterize the impact of urbanization and water infrastructure on urban hydrology (Bhaskar et al., 2016; Erban et al., 2018; Pangle et al., 2022). In this study, area-normalized I/I depth was compared with the precipitation and the area-normalized streamflow depths. The streamflow was

Table 3
Correlation Statistics Between Watershed Properties and Flow Regimes (Q_{10} , Q_{50} , Q_{90}) and Recession Parameters (Recession Slope, a , and Recession Exponent, b) of Streamflow

Variables	Metrics	Q_{10}	Q_{50}	Q_{90}	a	b
Imperviousness (All watersheds)	Slope	0.014	-0.005	-0.002	0.002	0.003
	R^2	0.38	0.37	0.14	0.65	0.03
	p	0.006	0.007	0.131	5.53e-5	0.521
Imperviousness (Urban watersheds)	Slope	0.020	-0.005	6.09e-4	0.001	0.014
	R^2	0.653	0.44	0.04	0.37	0.31
	p	0.008	0.052	0.604	0.080	0.119
Sewer density (Urban watersheds)	Slope	0.037	-0.010	-0.001	0.004	7.4e-4
	R^2	0.61	0.55	0.05	0.67	2.5e-4
	p	0.013	0.022	0.580	0.007	0.968
Combined (Urban watersheds)	R^2	0.74	0.59	0.30	0.68	0.61
	p	0.018	0.070	0.340	0.034	0.059

Note. Contents with different shades refer to correlations with different levels of statistical significance. Dark gray: significant with $p \leq 0.01$; Light gray: significant with $0.01 < p \leq 0.05$; Bold text: marginally significant with $0.05 < p \leq 0.10$; White: not significant with $p > 0.10$.

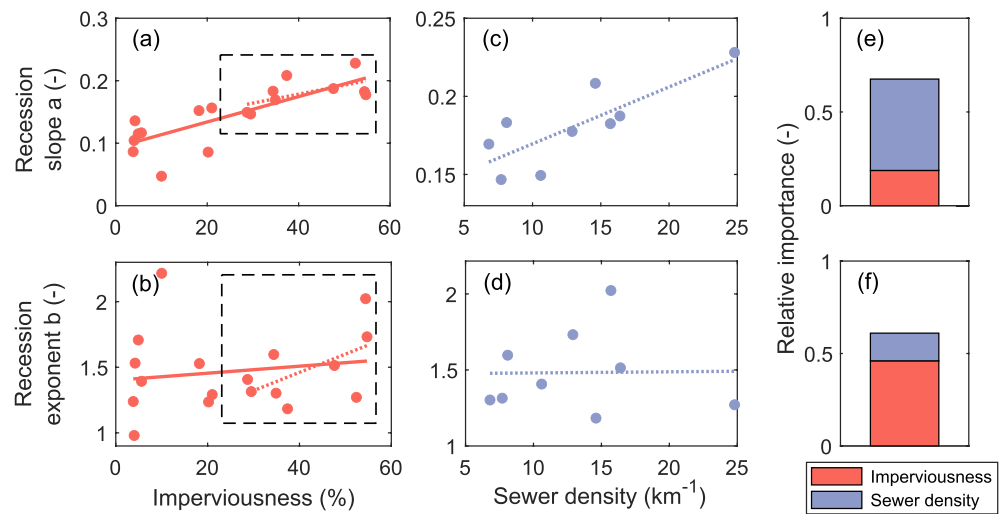


Figure 11. Relationship between watershed variables, that is, (a), (b) imperviousness and (c), (d) sanitary sewer density, and recession parameters, that is, (a), (c) recession slope, a and (b), (d) recession exponent, b . Panels (a), (b) include all watersheds; (c), (d) include the 9 urban watersheds with digitized sanitary sewer network data, denoted by the black rectangles in panels (a), (b). Panels (e), (f) show the variance of correlation attributed to imperviousness and sanitary sewer density based on dominance analysis performed solely on 9 urban watersheds.

normalized by the watershed area whereas the I/I was normalized by the sewershed area. Thus, the actual I/I depths in the watersheds can be lower than those in the sewersheds due to lower sewer density. The median area-normalized I/I depth (296 mm) was on the same order of magnitude as the measured precipitation (867 mm) and streamflow (424 mm) (Figure 5). In some sewersheds, the I/I depth was even close to precipitation (830 vs. 867 mm). This large spatial variability of I/I depths could come from the inter-sewershed differences in imperviousness, groundwater level, density of sanitary sewers, and proportion of rooftops with direct connection to sanitary sewers, etc. The I/I depth relative to the other water fluxes was similar to estimates in Baltimore (precipitation 1,160 mm, I/I 565 mm) (Bhaskar & Welty, 2012). In contrast, the I/I depth estimated for 4 watersheds in Atlanta was an order of magnitude smaller than the depths estimated for Milwaukee and Baltimore (~ 30 –51 mm), although precipitation was similar (1,143 mm) (Pangle et al., 2022). The sanitary sewer density in Atlanta was lower than in Milwaukee (7.5–9.0 km⁻¹ vs. 6.8–24.8 km⁻¹), which may explain the large difference in I/I . In addition, the difference in I/I depth could also be attributable to differences in water table depths. While we lack data on water table dynamics in the study sites, the relative depth of the phreatic surface determines the fraction (and duration of inundation) of pipes that are inundated and is an important factor determining I/I response to precipitation.

As shown here, I/I can be a large component of the water balance. The sewershed-area-normalized depths of I/I were similar in magnitude as similarly normalized depths of precipitation in some sewersheds. Considering that ET and recharge emanating from these sewersheds are not zero, such results seemingly imply a negative imbalance between outfluxes and influxes. However, it is important to recall that some I/I measured at the outlet of a delineated sewershed may include water derived from sources outside of that delineated area. Such unaccounted for fluxes are common in urban areas throughout the United States (Li et al., 2020). Additional sources of I/I may include net decline of stored groundwater or unaccounted water sources within the catchment such as leakage from water distribution systems and urban irrigation (Bhaskar & Welty, 2012; Bhaskar et al., 2016; Fillo et al., 2021; Lancia et al., 2020; Lerner, 2002; Sanzana et al., 2019; Tennant et al., 2021). There is evidence showing that the groundwater table in urban Milwaukee is dropping over time in recent years (Choi et al., 2012). In Milwaukee, 19%–22% of finished drinking water leaked from the distribution system between 2017 and 2020 (Milwaukee Water Works, 2020), representing 63–82 mm when averaged over the entire service area. During the same period, approximately 12% of end water use is for urban irrigation, representing 40–44 mm for the entire service area. Therefore, up to 40% of I/I could be derived from drinking water leakage and urban irrigation in this system, leaving additional sources to be quantified. An additional source may be lateral groundwater sourced from areas outside the sewershed delineated by the sewer network, which could not be estimated here. There is

no data to support this possibility. But if this is the case, it reflects a phenomenon that leaky sewers, because of I/I, are draining a larger subsurface drainage area compared to the surface sewershed area. In addition, the uncertainty and spatial variability in different hydrologic fluxes (e.g., precipitation and ET) can also contribute to this negative net annual balance of inflows and outflows.

As shown in this study, there is great uncertainty in quantifying water fluxes, especially in urban watersheds with infrastructure fluxes such as I/I. We recognize the existence of these uncertainties, leave the water balance open, and ask for further efforts to identify the unknown water fluxes (Kampf et al., 2020).

4.2. I/I Control on Streamflow Regimes

In this study, we found evidence that subsurface drainage via I/I may be an important contributor to streamflow “flashiness” in urban streams, in addition to imperviousness. Most prior studies attributed flashiness to expanded impervious cover (Molina et al., 2015; Rosburg et al., 2017; Rose & Peters, 2001; Shuster et al., 2005), while one modeling study identified the effect of I/I (Bhaskar et al., 2015). Our results showed that land cover change and subsurface drainage, representing major urbanization signatures, explained most of the flow regime distortions in high and intermediate flows. Their statistical contributions were comparable for high flows (39.1% and 34.5%), while subsurface drainage contributed more to intermediate flows (35.0% vs. 23.7%) (Figure 11). However, we did not detect any correlations with low flows in this study. This result therefore differed from existing studies which detected low flow reduction by I/I, for example, in Long Island, NY (Plunhowski & Spinello, 1978; Simmons & Reynolds, 1982), Baltimore, MD (Bhaskar et al., 2015), and Atlanta, GA (Diem et al., 2021; Pangle et al., 2022). The lack of an effect on baseflow could be further evidence that I/I in our study area originated from other non-stream sources.

4.3. I/I Control on Stream Baseflow Recession Rate

The I/I baseflow recession rate was slower than streamflow, which can be explained by dominance of groundwater inputs. This substantial amount of baseflow discharge through I/I may contribute to the commonly observed quicker baseflow recession in urban streams (Bhaskar & Welty, 2015; Bonneau et al., 2018; Burns et al., 2005; Konrad, 2016; Rose & Peters, 2001). The contrasting baseflow recession rates in urban and reference watersheds are likely driven by the combined effects of imperviousness, I/I, and differences in vegetation cover, soil depth and horizonation, and ET.

Subsurface drainage explained more of the variation in a (49%) than land cover change (19%), suggesting subsurface drainage via I/I as the primary control on baseflow recession. Watersheds with denser sewers have larger contact area with the subsurface, which facilitates drainage and accelerates the reduction of baseflow during dry periods (Marani et al., 2001; Price et al., 2011). In a modeling study, I/I was found to be the primary control on subsurface storage, which is proportional to baseflow recession rate, in urban watersheds in Baltimore (Bhaskar et al., 2015). In addition to I/I, recession rate may also be attributed to differences in watershed geology (Hopkins et al., 2015), ET, and other urbanization interventions (e.g., groundwater withdrawal, urban soil modifications) (Bonneau et al., 2018).

4.4. Contrasting Recession Nonlinearity Between I/I and Streamflow

The I/I baseflow recession was more nonlinear than streamflow in the urban watersheds (Figure 10). High I/I recession nonlinearity may be explained by unique features of urban soils and sewer networks, including high heterogeneity in soil properties and the locations of sewer network defects, as well as the geometry of the sewer network structure. The recession exponent has been theoretically linked with soil hydraulic property heterogeneity (Harman et al., 2009) and the geomorphic structure of drainage networks (Biswal & Marani, 2010, 2014). Urban soils are highly heterogeneous (De Kimpe & Morel, 2000; Greinert, 2015; Herrmann et al., 2018) and soils in proximity to sewers can be especially heterogeneous due to trenching and backfilling (Sharp, 2010). Further, sewer networks have a dendritic structure similar to stream networks (Krueger et al., 2017; Yang et al., 2017), but I/I inflows are spatially heterogeneous. Zhao et al. (2020) found that 7.9% of the sewers contributed 58% of the groundwater inflow in the sewer systems. Differences in recession nonlinearity between I/I and streamflow are likely due to the combination of these three factors and future studies on urban soil heterogeneity, network structure, and their impacts on storage-discharge properties of watersheds are warranted.

5. Conclusions

Inflow and infiltration (I/I) into sanitary sewers substantially affects urban hydrology yet remains a poorly quantified component of water balances. This study utilized an automatic approach to separate I/I from sanitary sewer flow based on autoregressive modeling and recursive digital filters. We then combined this estimate of I/I with nearby streamflow records to quantify the fraction of urban water balance discharged through I/I, analyzed and compared the hydrograph and recession characteristics of I/I and streamflow in urban and reference watersheds, and further investigated the impact of I/I on streamflow recession.

I/I exhibited a major role in urban hydrology in our study area of Milwaukee, Wisconsin, USA, given the comparable area-normalized depths between I/I, precipitation, and streamflow. In particular, during winter and spring, I/I commonly exceeded precipitation, while exceeding urban streamflow for much of the year. I/I had greater median and low flows than urban streamflow with more temporally consistent I/I flow compared to streamflow. Thus, I/I not only reduced the low flows, but also distorted the flow regime, increasing streamflow flashiness. I/I recession was slower and more nonlinear than urban streamflow recession. The lower baseflow recession rate of I/I was caused by high dominance and temporal consistency of groundwater inflow, while high nonlinearity may be attributed to sewer network structure or heterogeneity in soil type and sewer defects.

Across all streams, high flows increased, intermediate flows decreased, and recession rate increased with imperviousness and sanitary sewer density. Imperviousness and sanitary sewer density contributed comparably to high flow regimes, while sewer density dominated the intermediate flow regimes and baseflow recession rate over imperviousness. Sanitary sewer density explained 35% of the variability in intermediate flows and 49% of variability in baseflow recession rates, whereas imperviousness only explained 24% of intermediate flow variability and 19% of baseflow recession variability.

This study highlights the necessity of including the impact of subsurface drainage and I/I when considering the effects of urbanization on hydrology. An important next step could be to perform a larger-scale meta-analysis on the impact of subsurface drainage on urban streamflow regime. Additional studies could also focus on better understanding urban soil heterogeneity and its impact on storage-discharge properties of watersheds, and studies of sanitary sewer morphology and its controls on I/I and streamflow recession. With such efforts, the key processes in urban water balances and the governing factors for flow regimes in urban watersheds can be better understood.

Data Availability Statement

The streamflow data used in this study is collected by the United States Geologic Survey (USGS). The sanitary sewer flow data used in this study is collected by Milwaukee Metropolitan Sewer District. All the data can be accessed from Zhang et al. (2023).

References

- Arnold, J. G., Allen, P. M., Muttiyah, R., & Bernhardt, G. (1995). Automated base flow separation and recession analysis techniques. *Groundwater*, 33(6), 1010–1018. <https://doi.org/10.1111/j.1745-6584.1995.tb00046.x>
- Barron, O. V., Barr, A. D., & Donn, M. J. (2013). Effect of urbanization on the water balance of a catchment with shallow groundwater. *Journal of Hydrology*, 485, 162–176. <https://doi.org/10.1016/j.jhydrol.2012.04.027>
- Beheshti, M., & Sægvog, S. (2018). Sustainability assessment in strategic management of wastewater transport system: A case study in Trondheim, Norway. *Urban Water Journal*, 15(1), 1–8. <https://doi.org/10.1080/1573062x.2017.1363253>
- Beighley, R. E., Melack, J. M., & Dunne, T. (2003). Impacts of California's climatic regimes and coastal land use change on streamflow characteristics. *Journal of the American Water Resources Association*, 39(6), 1419–1433. <https://doi.org/10.1111/j.1752-1688.2003.tb04428.x>
- Bentes, I., Silva, D., Vieira, C., & Matos, C. (2022). Inflow quantification in urban sewer networks. *Hydrology*, 9(4), 52. <https://doi.org/10.3390/hydrology9040052>
- Bhaskar, A. S., Beesley, L., Burns, M. J., Fletcher, T. D., Hamel, P., Oldham, C. E., & Roy, A. H. (2016). Will it rise or will it fall? Managing the complex effects of urbanization on base flow. *Freshwater Science*, 35(1), 293–310. <https://doi.org/10.1086/685084/>
- Bhaskar, A. S., Hopkins, K. G., Smith, B. K., Stephens, T. A., & Miller, A. J. (2020). Hydrologic signals and surprises in U.S. Streamflow records during urbanization. *Water Resources Research*, 56(9), e2019WR027039. <https://doi.org/10.1029/2019WR027039>
- Bhaskar, A. S., & Welty, C. (2012). Water balances along an urban-to-rural gradient of Metropolitan Baltimore, 2001–2009. *Environmental and Engineering Geoscience*, 18(1), 37–50. <https://doi.org/10.2113/gsegeosci.18.1.37>
- Bhaskar, A. S., & Welty, C. (2015). Analysis of subsurface storage and streamflow generation in urban watersheds. *Water Resources Research*, 51(3), 1493–1513. <https://doi.org/10.1002/2014WR015607>
- Bhaskar, A. S., Welty, C., Maxwell, R. M., & Miller, A. J. (2015). Untangling the effects of urban development on subsurface storage in Baltimore. *Water Resources Research*, 51(2), 1158–1181. <https://doi.org/10.1002/2014WR016039>

Acknowledgments

The authors acknowledge the Industry-University Cooperative Research Center (I/UCRC) for financial support and the Milwaukee Metropolitan Sewerage District (MMSD) for help in providing the sanitary sewer flow data and digitized sanitary sewer pipes data. Funding for this work was provided in part by the Virginia Agricultural Experiment Station and the Hatch Program of the National Institute of Food and Agriculture, U.S. Department of Agriculture (Multi-state Project W4188 and Hatch Project 1026126).

- Biswal, B., & Marani, M. (2010). Geomorphological origin of recession curves. *Geophysical Research Letters*, 37(24), 24403. <https://doi.org/10.1029/2010GL045415>
- Biswal, B., & Marani, M. (2014). 'Universal' recession curves and their geomorphological interpretation. *Advances in Water Resources*, 65, 34–42. <https://doi.org/10.1016/j.advwatres.2014.01.004>
- Bonneau, J., Burns, M. J., Fletcher, T. D., Witt, R., Drysdale, R. N., & Costelloe, J. F. (2018). The impact of urbanization on subsurface flow paths—A paired-catchment isotopic study. *Journal of Hydrology*, 561, 413–426. <https://doi.org/10.1016/j.jhydrol.2018.04.022>
- Brandes, D., Cavallo, G. J., & Nilson, M. L. (2005). Base flow trends in urbanizing watersheds of the Delaware River basin. *Journal of the American Water Resources Association*, 41(6), 1377–1391. <https://doi.org/10.1111/j.1752-1688.2005.tb03806.x>
- Braud, I., Breil, P., Thollet, F., Lagouy, M., Branger, F., Jacquemint, C., et al. (2013). Evidence of the impact of urbanization on the hydrological regime of a medium-sized periurban catchment in France. *Journal of Hydrology*, 485, 5–23. <https://doi.org/10.1016/j.jhydrol.2012.04.049>
- Brutsaert, W., & Nieber, J. L. (1977). Regionalized drought flow hydrographs from a mature glaciated plateau. *Water Resources Research*, 13(3), 637–643. <https://doi.org/10.1029/WR013I003P00637>
- Budescu, D. V. (1993). Dominance analysis: A new approach to the problem of relative importance of predictors in multiple regression. *Psychological Bulletin*, 114(3), 542–551. <https://doi.org/10.1037/0033-2909.114.3.542>
- Burns, D., Vitvar, T., McDonnell, J., Hassett, J., Duncan, J., & Kendall, C. (2005). Effects of suburban development on runoff generation in the Croton River basin, New York, USA. *Journal of Hydrology*, 311(1–4), 266–281. <https://doi.org/10.1016/j.jhydrol.2005.01.022>
- Choi, W., Galasinski, U., Cho, S. J., & Hwang, C. S. (2012). A spatiotemporal analysis of groundwater level changes in relation to urban growth and groundwater recharge potential for Waukesha County, Wisconsin. *Geographical Analysis*, 44(3), 219–234. <https://doi.org/10.1111/J.1538-4632.2012.00848.X>
- Debbage, N., & Shepherd, J. M. (2018). The influence of urban development patterns on streamflow characteristics in the Charlanta Megaregion. *Water Resources Research*, 54(5), 3728–3747. <https://doi.org/10.1029/2017WR021594>
- De Kimpe, C. R., & Morel, J. L. (2000). Urban soil management: A growing concern. *Soil Science*, 165(1), 31–40. <https://doi.org/10.1097/00010694-200001000-00005>
- Dewitz, J., & U.S. Geological Survey. (2021). *National land cover database (NLCD) 2019 products (version 2.0, June 2021)*. U.S. Geological Survey Data Release. <https://doi.org/10.5066/P96HHBIE>
- Diem, J. E., Pangle, L. A., Milligan, R. A., & Adams, E. A. (2021). Intra-annual variability of urban effects on streamflow. *Hydrological Processes*, 35(9), e14371. <https://doi.org/10.1002/hyp.14371>
- Dirckx, G., Van Daele, S., & Hellinck, N. (2016). Groundwater Infiltration Potential (GWIP) as an aid to determining the cause of dilution of wastewater. *Journal of Hydrology*, 542, 474–486. <https://doi.org/10.1016/j.jhydrol.2016.09.020>
- DNR. (1999). Bureau for remediation and redevelopment tracking system (BRRTS) on the web Wisconsin DNR. Retrieved from <https://dnr.wisconsin.gov/topic/Brownfields/botw.html>
- Dralle, D. N., Karst, N. J., Charalampous, K., Veenstra, A., & Thompson, S. E. (2017). Event-scale power law recession analysis: Quantifying methodological uncertainty. *Hydrology and Earth System Sciences*, 21(1), 65–81. <https://doi.org/10.5194/hess-21-65-2017>
- Eckhardt, K. (2005). How to construct recursive digital filters for baseflow separation. *Hydrological Processes*, 19(2), 507–515. <https://doi.org/10.1002/hyp.5675>
- Eiswirth, M., & Hötzl, H. (1997). The impact of leaking sewers on urban groundwater. *Groundwater in the Urban Environment*, 399–404. http://users.ipfw.edu/isiorho/G300Eiswirth-Hoetzl_IAH_Nottingham_1997.pdf
- Ellis, J. B., & Bertrand-Krajewski, J. L. (2010). Assessing infiltration and exfiltration on the Performance of Urban Sewer Systems (APUSS). *Water Intelligence Online*, 9. <https://doi.org/10.2166/9781780401652>
- Erban, L. E., Balogh, S. B., Campbell, D. E., & Walker, H. A. (2018). An R package for open, reproducible analysis of urban water systems, with application to Chicago. *Open Water*, 5(1), 26–40. <https://scholarsarchive.byu.edu/openwater/vol5/iss1/3/>
- Fillo, N. K., Bhaskar, A. S., & Jefferson, A. J. (2021). Lawn irrigation contributions to semi-arid urban baseflow based on water-stable isotopes. *Water Resources Research*, 57(8), e2020WR028777. <https://doi.org/10.1029/2020WR028777>
- Finkenbine, J. K., Atwater, J. W., & Mavinic, D. S. (2000). Stream health after urbanization. *Journal of the American Water Resources Association*, 36(5), 1149–1160. <https://doi.org/10.1111/j.1752-1688.2000.tb05717.x>
- Greinert, A. (2015). The heterogeneity of urban soils in the light of their properties. *Journal of Soils and Sediments*, 15(8), 1725–1737. <https://doi.org/10.1007/s11368-014-1054-6/>
- Grimmond, C. S. B., & Oke, T. R. (1991). An evapotranspiration-interception model for urban areas. *Water Resources Research*, 27(7), 1739–1755. <https://doi.org/10.1029/91WR00557>
- Grimmond, C. S. B., & Oke, T. R. (1999). *Evapotranspiration rates in urban areas* (Vol. 259, pp. 235–243). IAHS-AISH Publication.
- Haase, D. (2009). Effects of urbanisation on the water balance—A long-term trajectory. *Environmental Impact Assessment Review*, 29(4), 211–219. <https://doi.org/10.1016/j.eiar.2009.01.002>
- Hardison, E. C., O'Driscoll, M. A., Deloatch, J. P., Howard, R. J., & Brinson, M. M. (2009). Urban land use, channel incision, and water table decline along coastal plain streams, North Carolina'. *JAWRA Journal of the American Water Resources Association*, 45(4), 1032–1046. <https://doi.org/10.1111/J.1752-1688.2009.00345.X>
- Harman, C. J., Sivapalan, M., & Kumar, P. (2009). Power law catchment-scale recessions arising from heterogeneous linear small-scale dynamics. *Water Resources Research*, 45(9), 9404. <https://doi.org/10.1029/2008WR007392>
- Herrmann, D. L., Schifman, L. A., & Shuster, W. D. (2018). Widespread loss of intermediate soil horizons in urban landscapes. *Proceedings of the National Academy of Sciences of the United States of America*, 115(26), 6751–6755. <https://doi.org/10.1073/pnas.1800305115>
- Hopkins, K. G., Morse, N. B., Bain, D. J., Bettez, N. D., Grimm, N. B., Morse, J. L., et al. (2015). Assessment of regional variation in stream-flow responses to urbanization and the persistence of physiography. *Environmental Science and Technology*, 49(5), 2724–2732. <https://doi.org/10.1021/es505389y>
- Kampf, S. K., Burges, S. J., Hammond, J. C., Bhaskar, A., Covino, T. P., Eurich, A., et al. (2020). The case for an open water balance: Re-envisioning network design and data analysis for a complex, uncertain world. *Water Resources Research*, 56(6), e2019WR026699. <https://doi.org/10.1029/2019WR026699>
- Kokkonen, T. V., Grimmond, C. S. B., Christen, A., Oke, T. R., & Järvi, L. (2018). Changes to the water balance over a century of urban development in two neighborhoods: Vancouver, Canada. *Water Resources Research*, 54(9), 6625–6642. <https://doi.org/10.1029/2017WR022445>
- Konrad, C. P. (2016). Effects of urban development on floods. U.S. Geological Survey Fact Sheet 076-03 Retrieved from <https://pubs.usgs.gov/fs/fs07603/>
- Kracht, O., Gresch, M., & Gujer, W. (2007). A stable isotope approach for the quantification of sewer infiltration. *Environmental Science and Technology*, 41(16), 5839–5845. <https://doi.org/10.1021/es062960c>

- Kraha, A., Turner, H., Nimon, K., Zientek, L. R., & Henson, R. K. (2012). Tools to support interpreting multiple regression in the face of multicollinearity. *Frontiers in Psychology*, 3, 44. <https://doi.org/10.3389/fpsyg.2012.00044>
- Kroll, C. N., & Song, P. (2013). Impact of multicollinearity on small sample hydrologic regression models. *Water Resources Research*, 49(6), 3756–3769. <https://doi.org/10.1002/wrcr.20315>
- Krueger, E., Klinkhamer, C., Ulrich, C., Zhan, X., & Rao, P. S. C. (2017). Generic patterns in the evolution of urban water networks: Evidence from a large Asian city. *Physical Review E*, 95(3), 032312. <https://doi.org/10.1103/PhysRevE.95.032312>
- Lancia, M., Zheng, C., He, X., Lerner, D. N., & Andrews, C. (2020). Groundwater complexity in urban catchments: Shenzhen, southern China. *Groundwater*, 58(3), 470–481. <https://doi.org/10.1111/gwat.12935>
- Lerner, D. N. (2002). Identifying and quantifying urban recharge: A review. *Hydrogeology Journal*, 10(1), 143–152. <https://doi.org/10.1007/s10040-001-0177-1>
- Li, C., Sun, G., Caldwell, P. V., Cohen, E., Fang, Y., Zhang, Y., et al. (2020). Impacts of urbanization on watershed water balances across the conterminous United States. *Water Resources Research*, 56(7), e2019WR026574. <https://doi.org/10.1029/2019WR026574>
- Marani, M., Eltahir, E., & Rinaldo, A. (2001). Geomorphic controls on regional base flow. *Water Resources Research*, 37(10), 2619–2630. <https://doi.org/10.1029/2000WR000119>
- Mejía, A., Rossel, F., Gironás, J., & Jovanovic, T. (2015). Anthropogenic controls from urban growth on flow regimes. *Advances in Water Resources*, 84, 125–135. <https://doi.org/10.1016/j.advwatres.2015.08.010>
- Milwaukee Water Works. (2020). Water, electric, or joint utility annual report. Retrieved from <https://city.milwaukee.gov/ImageLibrary/Groups/WaterWorks/files/Annual-Reports/PSC2020Final.pdf>
- Molina, A., Vanacker, V., Brisson, E., Mora, D., & Balthazar, V. (2015). Multidecadal change in streamflow associated with anthropogenic disturbances in the tropical Andes. *Hydrology and Earth System Sciences*, 19(10), 4201–4213. <https://doi.org/10.5194/hess-19-4201-2015>
- O'Driscoll, M., Clinton, S., Jefferson, A., Manda, A., & McMillan, S. (2010). Urbanization effects on watershed hydrology and in-stream processes in the southern United States. *Water (Switzerland)*, 2(3), 605–648. <https://doi.org/10.3390/w2030605>
- Oswald, C. J., Kelleher, C., Ledford, S. H., Hopkins, K. G., Sytsma, A., Tetzlaff, D., et al. (2023). Integrating urban water fluxes and moving beyond impervious surface cover: A review. *Journal of Hydrology*, 618, 129188. <https://doi.org/10.1016/j.jhydrol.2023.129188>
- Pangle, L. A., Diem, J. E., Milligan, R., Adams, E., & Murray, A. (2022). Contextualizing inflow and infiltration within the streamflow regime of urban watersheds. *Water Resources Research*, 58(1), e2021WR030406. <https://doi.org/10.1029/2021WR030406>
- Pawlowski, C. W., RheaShuster, L. L. W. D., Barden, G., & Asce, M. (2013). Some factors affecting inflow and infiltration from residential sources in a core urban area: Case study in a Columbus, Ohio, neighborhood. *Journal of Hydraulic Engineering*, 140(1), 105–114. [https://doi.org/10.1061/\(ASCE\)HY.1943-7900.0000799](https://doi.org/10.1061/(ASCE)HY.1943-7900.0000799)
- Plunhowski, E. J., & Spinello, A. G. (1978). Impact of sewerage systems on stream base flow and ground-water recharge on long Island, New York. *Journal of Research of the U. S. Geological Survey*, 6(2), 263–271.
- Price, K. (2011). Effects of watershed topography, soils, land use, and climate on baseflow hydrology in humid regions: A review. *Progress in Physical Geography*, 35(4), 465–492. <https://doi.org/10.1177/0309133311420714>
- Price, K., Jackson, C. R., Parker, A. J., Reitan, T., Dowd, J., & Cyterski, M. (2011). Effects of watershed land use and geomorphology on stream low flows during severe drought conditions in the southern Blue Ridge Mountains, Georgia and North Carolina, United States. *Water Resources Research*, 47(2), W02516. <https://doi.org/10.1029/2010WR009340>
- Prigiobbe, V., & Giulianielli, M. (2009). Quantification of sewer system infiltration using $\delta^{18}\text{O}$ hydrograph separation. *Water Science and Technology*, 60(3), 727–735. <https://doi.org/10.2166/wst.2009.399>
- Rosburg, T. T., Nelson, P. A., & Bledsoe, B. P. (2017). Effects of urbanization on flow duration and stream flashiness: A case study of puget sound streams, western Washington, USA. *JAWRA Journal of the American Water Resources Association*, 53(2), 493–507. <https://doi.org/10.1111/1752-1688.12511>
- Rose, S., & Peters, N. E. (2001). Effects of urbanization on streamflow in the Atlanta area (Georgia, USA): A comparative hydrological approach. *Hydrological Processes*, 15(8), 1441–1457. <https://doi.org/10.1002/hyp.218>
- Sánchez-Murillo, R., Brooks, E. S., Elliot, W. J., Gazel, E., & Boll, J. (2015). Baseflow recession analysis in the inland Pacific Northwest of the United States. *Hydrogeology Journal*, 23(2), 287–303. <https://doi.org/10.1007/s10040-014-1191-4>
- Sanzana, P., Gironás, J., Braud, I., Muñoz, J. F., Vicuña, S., Reyes-Paecke, S., et al. (2019). Impact of urban growth and high residential irrigation on streamflow and groundwater levels in a peri-urban semiarid catchment. *JAWRA Journal of the American Water Resources Association*, 55(3), 720–739. <https://doi.org/10.1111/1752-1688.12743>
- Searcy, J. K. (1959). *Flow-duration curves*. Water Supply Paper. <https://doi.org/10.3133/WSP1542A>
- Sharp, J. M. (2010). The impacts of urbanization on groundwater systems and recharge. *Aquamundi*, 1, 51–56. <https://doi.org/10.4409/Am-004-10-0008>
- Shuster, W. D., Bonta, J., Thurston, H., Warnemuende, E., & Smith, D. R. (2005). Impacts of impervious surface on watershed hydrology: A review. *Urban Water Journal*, 2(4), 263–275. <https://doi.org/10.1080/15730620500386529>
- Simmons, D. L., & Reynolds, R. J. (1982). Effects of urbanization on base flow of selected south-shore streams, long Island, New York. *JAWRA Journal of the American Water Resources Association*, 18(5), 797–805. <https://doi.org/10.1111/j.1752-1688.1982.tb00075.x>
- Tennant, H., Neilson, B. T., Miller, M. P., & Xu, T. (2021). Ungaged inflow and loss patterns in urban and agricultural sub-reaches of the Logan River Observatory. *Hydrological Processes*, 35(4), e14097. <https://doi.org/10.1002/hyp.14097>
- United States Geological Survey. (2019). USGS water data for the nation. National Water Information System: Web Interface. Retrieved from <https://waterdata.usgs.gov/nwis>
- Vallabhaneni, S., Lai, F. H., Chan, C., Burgess, E. H., & Field, R. (2008). SSOAP—A USEPA toolbox for SSO analysis and control planning. In *World environmental and water resources congress 2008: Ahupua'a—Proceedings of the world environmental and water resources congress* (Vol. 316, pp. 1–10). [https://doi.org/10.1061/40976\(316\)24](https://doi.org/10.1061/40976(316)24)
- Vanderlyn, C., & Condren, A. (1990). *Rainfall induced infiltration into sewer systems*. US Environmental Protection Agency.
- Walsh, C. J., Roy, A. H., Feminella, J. W., Cottingham, P. D., Groffman, P. M., & Morgan, R. P. (2005). The urban stream syndrome: Current knowledge and the search for a cure. *Journal of the North American Benthological Society*, 24(3), 706–723. <https://doi.org/10.1899/04-028.1>
- Wang, D., & Cai, X. (2010). Recession slope curve analysis under human interferences. *Advances in Water Resources*, 33(9), 1053–1061. <https://doi.org/10.1016/j.advwatres.2010.06.010>
- Weiss, G., Brombach, H., & Haller, B. (2002). Infiltration and inflow in combined sewer systems: Long-term analysis. *Water Science and Technology*, 45(7), 11–19. <https://doi.org/10.2166/wst.2002.0112>
- Winter, T. C., Harvey, J. W., Franke, O. L., & Alley, W. M. (1998). *Ground water and surface water—A single resource—U.S. Geological Survey Circular 1139* (Vol. 1, p. 79). USGS Publications. Retrieved from <https://pubs.usgs.gov/circ/circ1139/>

- Wittenberg, H., & Sivapalan, M. (1999). Watershed groundwater balance estimation using streamflow recession analysis and baseflow separation. *Journal of Hydrology*, 219(1–2), 20–33. [https://doi.org/10.1016/S0022-1694\(99\)00040-2](https://doi.org/10.1016/S0022-1694(99)00040-2)
- Yang, S., Paik, K., McGrath, G. S., Ulrich, C., Krueger, E., Kumar, P., & Rao, P. S. C. (2017). Functional topology of evolving urban drainage networks. *Water Resources Research*, 53(11), 8966–8979. <https://doi.org/10.1002/2017WR021555>
- Zhang, K., & Parolari, A. J. (2022). Impact of stormwater infiltration on rainfall-derived inflow and infiltration: A physically based surface–subsurface urban hydrologic model. *Journal of Hydrology*, 610, 127938. <https://doi.org/10.1016/j.jhydrol.2022.127938>
- Zhang, K., Sebo, S., McDonald, W., Bhaskar, A. S., Shuster, W., Stewart, R. D., & Parolari, A. J. (2023). Data for “The role of inflow and infiltration (I/I) in urban water balances and streamflow regimes: A hydrograph analysis along the sewershed-watershed continuum” [Dataset]. <https://doi.org/10.4211/hs.c5a9a2fe41164ab092662526bbc1cbe3>
- Zhao, Z., Yin, H., Xu, Z., Peng, J., & Yu, Z. (2020). Pin-pointing groundwater infiltration into urban sewers using chemical tracer in conjunction with physically based optimization model. *Water Research*, 175, 115689. <https://doi.org/10.1016/j.watres.2020.115689>

References From the Supporting Information

- DeOreo, W. B., Mayer, P. W., Dziegielewski, B., & Kiefer, J. (2016). *Residential end uses of water, version 2*. Water Research Foundation. Retrieved from <https://www.waterrf.org/research/projects/residential-end-uses-water-version-2>
- Patnaik, S., Biswal, B., Kumar, D. N., & Sivakumar, B. (2015). Effect of catchment characteristics on the relationship between past discharge and the power law recession coefficient. *Journal of Hydrology*, 528, 321–328. <https://doi.org/10.1016/j.jhydrol.2015.06.032>